PROGRESS REPORT

PR 91565-430-3

For Month of September 1962

DEVELOPMENT OF AUXILIARY ELECTRIC
POWER SUPPLY SYSTEM

NASA Contract NAS 3-2550

Prepared by R. C. Thomas
R. C. Thomas

Approved by N. E. Morgan
N. E. Morgan
Group Supervisor
Space Power System

Approved by W. H. White
W. H. White
Engineering Manager
Power Systems

Aerospace Division
VICKERS INCORPORATED
Division of Sperry Rand Corporation
Torrance, California

INTRODUCTION

This report covers the work accomplished by Vickers Incorporated under NASA Contract NAS 3-2550 during the month of September, 1962. The objectives of this program are to conduct an engineering study culminating in the design of an electrical power generation system operating on hydrogen and oxygen in a space environment, and to conduct preliminary testing on critical system components.

PROGRAM SCHEDULE

The program schedule is shown in Fig. 1. The fabrication schedule has been delayed on the engine and regenerator to expedite work on the hydrogen compressor and oxygen injector. The resulting rescheduling will delay the development program on the experimental regenerator by approximately three weeks. It is planned to give priority to the hydrogen compressor and the oxygen injector since these components reflect the areas of greatest uncertainty. The program plan for this project covers the entries of Fig. 1 and was described in the progress report for July, 1962.

PARAMETRIC STUDIES

a. Cycle Analysis

The following assumptions have been used in cycle analysis studies to date:

1. Engine Speed = 4000 rpm
2. Oxygen/hydrogen ratio = 2.0
3. Diagram factor = 0.9 (for the case of zero

PROGRAM SCHEDULE NASA CONTRACT NAS 3-2550

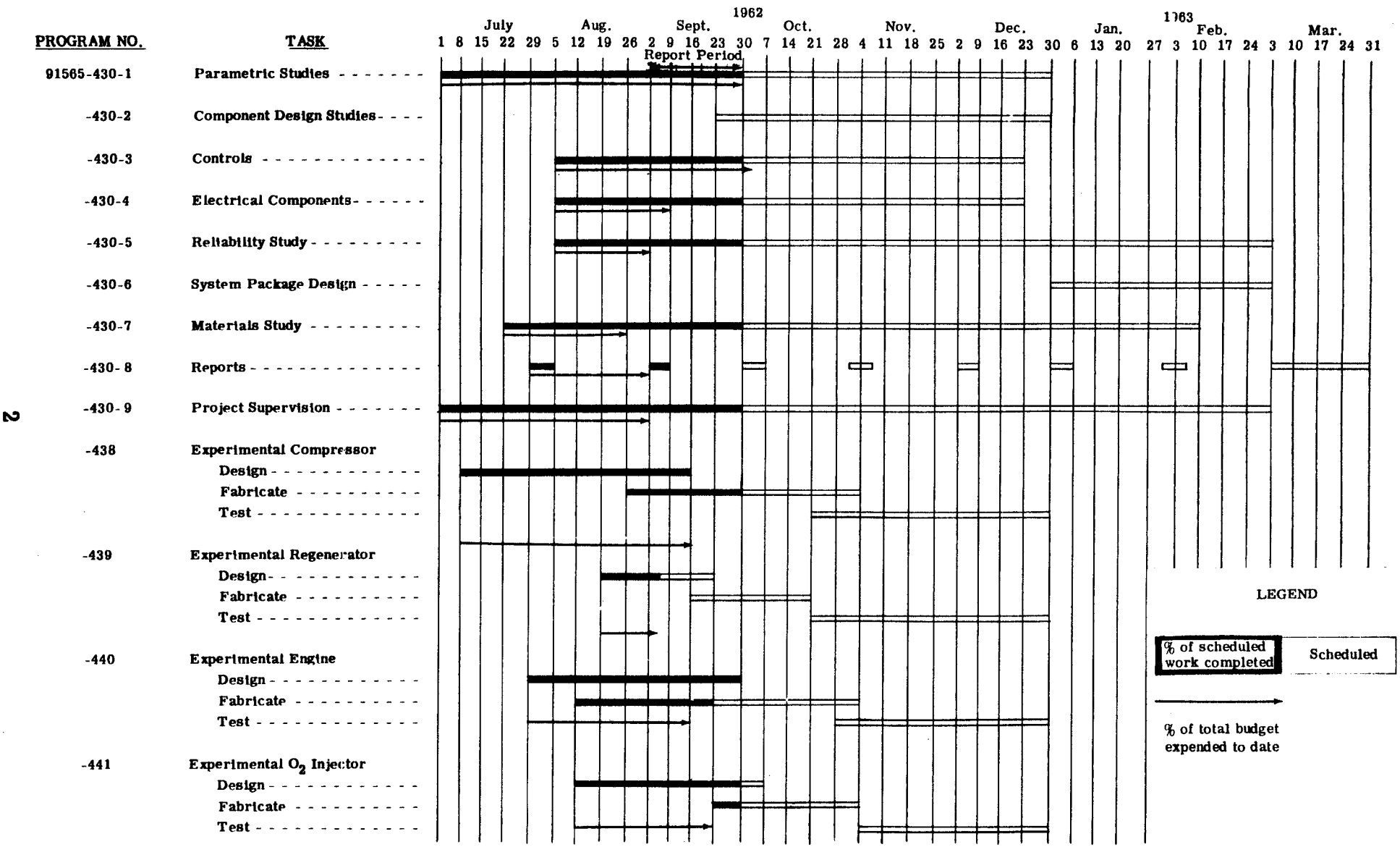

Fig. 1

heat rejection)

4. Maximum cylinder pressure = 1200 psi
5. Clearance volume = 5% (Except for the variable clearance volume study. This is the minimum practical limit.)
6. Friction Mean Effective Pressure (FMEP) = 11 psia
7. Constant volume combustion (at O_2/H_2 = 2.0 peak pressure is 3 times initial pressure).

The two external compression engine cycles under consideration are the throttled Otto cycle and the constant pressure - variable phase valve cycle. From a controls viewpoint the problems involved in either cycle are of the same order. For two engines in a redundant system the design BSPC for either cycle would be the same. Two Otto cycle engines sharing a 2 kw load equally would operate at a BSPC of 1.7 lb/kw hr. One constant pressure - variable phase cycle engine operating at 2 kw consumes 1.78 lb/kw hr. Therefore an engine choice cannot be made on an efficiency basis.

The variable phase engine is considerably smaller in size, yielding a lower system weight. However a larger engine has some scaling advantages.

The smaller variable phase engine operates at a much higher BMEP than the Otto cycle engine, which reduces its sensi-

tivity to back pressure. For example, at sea level the variable phase engine delivers 86.5% of its rated power in space, while the Otto cycle engine develops only 41% of its space power rating.

A more versatile engine capable of operating over a wider power range would result from a combination of the above two types of cycles; that is with a variable phase control in combination with the throttle control on the hydrogen inlet pressure. It is planned to study the combined cycle engine during the next report period.

Cryogenic Tankage - The system under development will require 1050 lbs. of propellant (700 lb. of oxygen and 350 lb. of hydrogen) for a 350 hour mission. Operation on boiloff from main propellant tanks for the first 100 hours will reduce the tankage requirements to 250 lbs. H_2 and 500 lbs. O_2. Supercritical storage appears to be the most practical method. It may be desirable to operate the engine directly on propellants supplied at critical pressure, disengaging the compressors after the first 100 hours.

The influence of hydrogen storage pressure on engine performance is now being investigated. Fig. 2 shows BSPC vs. maximum combustion pressure for an Otto cycle engine at maximum power. For an O_2/H mixture ratio of 2:1 the maximum combustion pressure is approximately three times the hydrogen inlet pressure. To lower hydrogen inlet pressure from 400 psi (fixed by maximum allowable cylinder pressure) to 300 psi (a practical supply pressure from a supercritical tank) entails a BSPC increase of 4%. This is a weight penalty of only 30 lbs. of propellant on a 350 hour mission.

Fig. 2

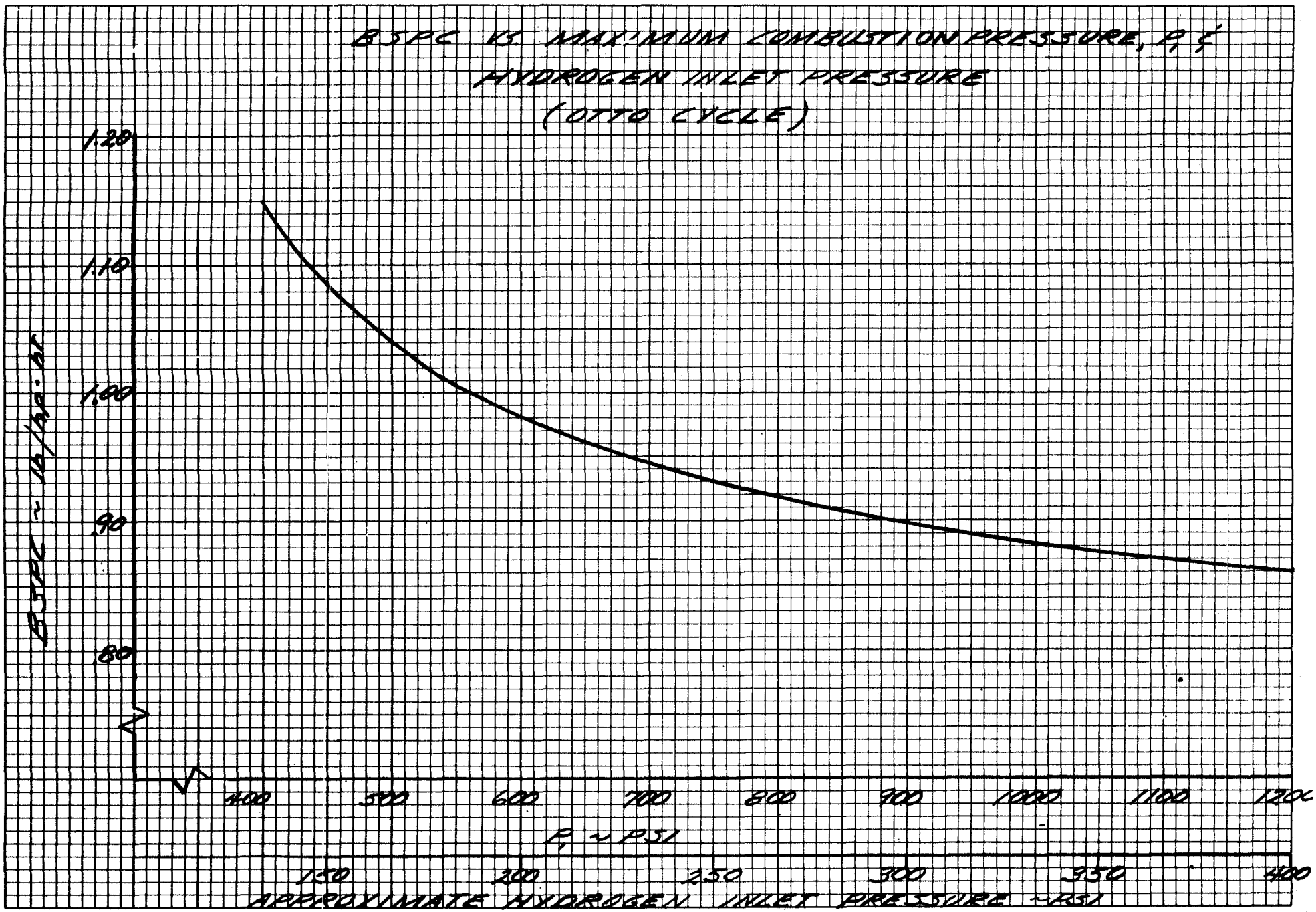
B.S.F.C. VS. MAXIMUM COMBUSTION PRESSURE, P, & HYDROGEN INLET PRESSURE
(OTTO CYCLE)
B.S.F.C. ~ lb/hp-hr
1.20
1.10
1.00
.90
.80
400
500
600
700
800
900
1000
1100
1200
P, ~ PSI
150
200
250
300
350
400
APPROXIMATE HYDROGEN INLET PRESSURE ~ PSI

Although subcritical storage might make possible a lower tank weight, proven liquid expulsion methods do not yet exist for zero-g operation. Also the tank weight saving due to lower internal pressure might be negated by tankage structural requirements necessary to withstand the shock of a lunar landing, or by greater insulation requirements than for supercritical tanks.

Supercritical storage is presently favored. The tankage investigation is being continued. The major source of information has been reference 1.

Compressor Analysis - Compressor work curves for saturated vapor inlet are presented in Figs. 3 and 4. Compression work is based on an inlet pressure of 15 psi. The hydrogen is compressed to 1200 psi and the oxygen to 1500 psi. These conditions represent the maximum work which the compressors will be required to perform.

Hydrogen compression work was calculated from a temperature entropy diagram for hydrogen, assuming 75% compressor efficiency. Oxygen compression work was calculated from the following expression:

$$(1) \quad W_{ORK_{ACTUAL}} = \frac{T_{IN}\, C_p \left[1 - \left(P_2/P_1\right)^{\frac{\gamma-1}{\gamma}}\right] \times 778}{\eta_c}$$

using the following numerical values:

$\eta_c = .80$, $C_p = .218$ BTU/LB·F., $\gamma = 1.4$.

Compression power as a function of engine power for various BSPC's is given in Fig. 5. This analysis is conservative. Actual values cannot be estimated until compressor design

Fig. 3

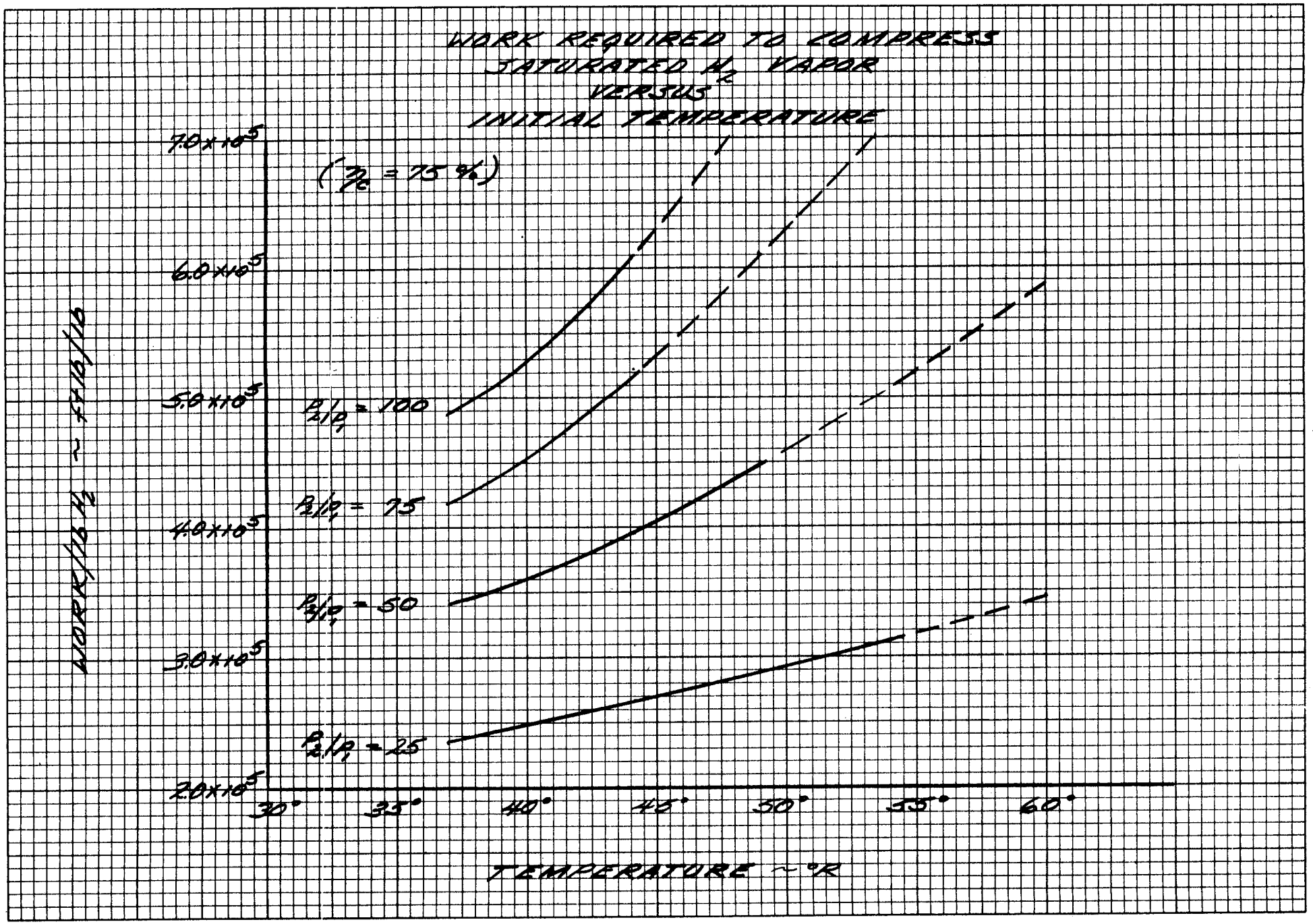
WORK REQUIRED TO COMPRESS
SATURATED H_2 VAPOR
VERSUS
INITIAL TEMPERATURE
(η_c = 75 %)
7.0×10^5
6.0×10^5
5.0×10^5
4.0×10^5
3.0×10^5
2.0×10^5
P_2/P_1 = 100
P_2/P_1 = 75
P_2/P_1 = 50
P_2/P_1 = 25
WORK/lb H_2 ~ ft-lb/lb
30°
35°
40°
45°
50°
55°
60°
TEMPERATURE ~ °R

Fig. 4

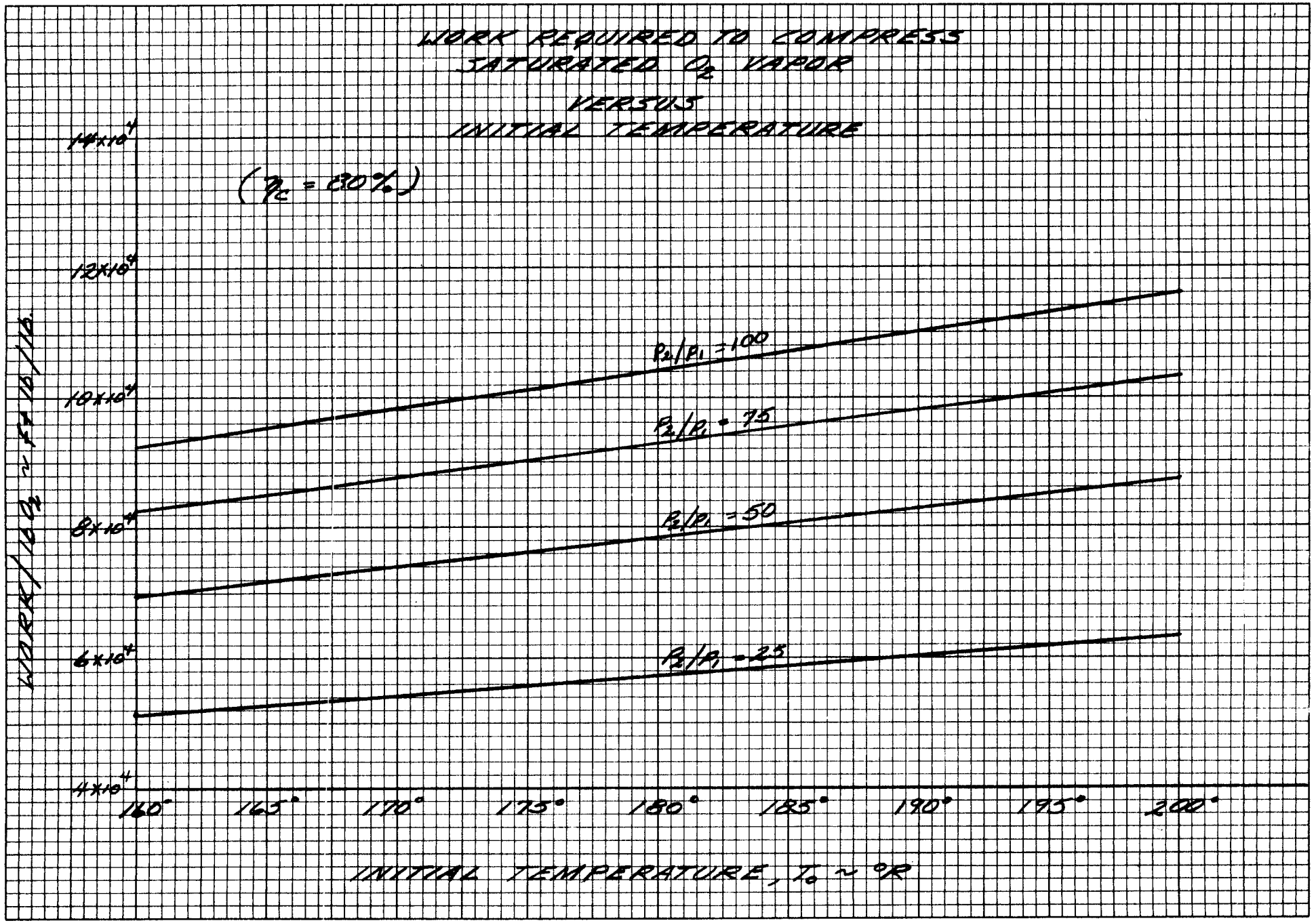
WORK REQUIRED TO COMPRESS
SATURATED O_2 VAPOR
VERSUS
INITIAL TEMPERATURE
(η_c = 80%)
14×10⁴
12×10⁴
10×10⁴
8×10⁴
6×10⁴
4×10⁴
WORK, ft lb / lb. O_2
P_2/P_1 = 100
P_2/P_1 = 75
P_2/P_1 = 50
P_2/P_1 = 25
160°
165°
170°
175°
180°
185°
190°
195°
200°
INITIAL TEMPERATURE, T_0 ~ °R

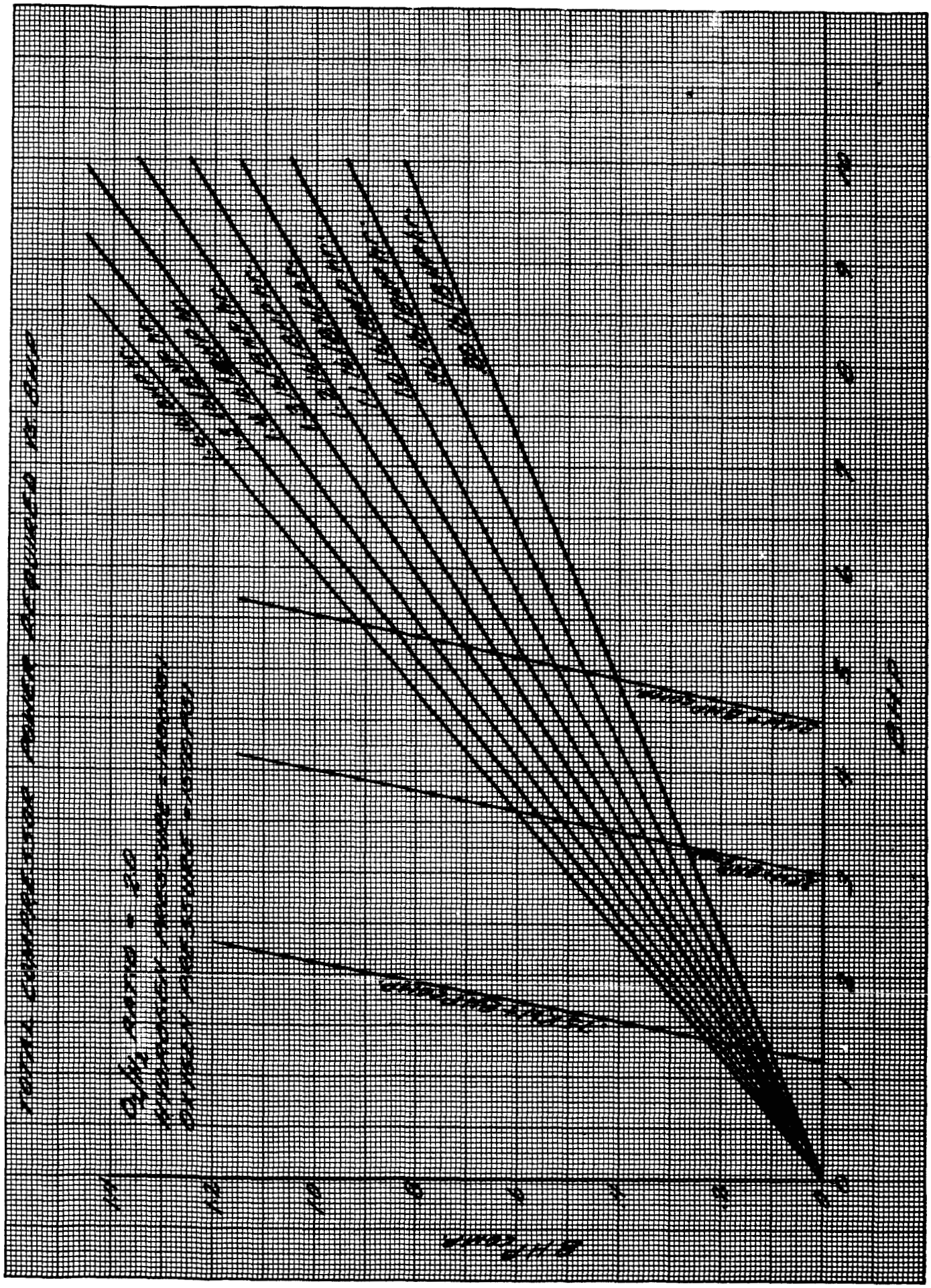

Fig. 5

is fixed. The three steep lines in Fig. 5 represent compressor vs. engine power for alternator outputs of .75, 2, and 3 kw respectively. These lines would be vertical for zero compressor work.

b. Heat Rejection Analysis

The Vickers Hydrox engine has two inherent and unavoidable factors which deviate from conventional engines. These are small cylinder size and a working fluid which is primarily hydrogen gas. Both of these factors tend to increase heat rejection per unit of power delivered. In recognition of this, the test engine was designed to permit use of heat dams in the cylinder head and piston crown, with the intake valve isolated from the combustion zone by stratification.

An analysis of the heat rejection characteristics of engines is presented using methods suggested in Reference 3. Heat rejection is a function of the following parameters:

(1) $$\frac{Q}{HP} \approx \frac{hA\,\Delta T}{PVB^2} \approx \frac{K/B\,(\frac{\rho VB}{\mu})^{.75} B^2 \Delta T}{PVB^2}$$

where h is film coefficient, A is piston area, Q is rate of heat transfer, T is temperature, B is cylinder bore, K is conductivity, μ is viscosity, V is piston speed, ρ is density, P is pressure, HP is power output.

(2) $$\frac{\rho VD}{\mu} = \frac{PVB}{RT\mu}$$

thus:

(3) $$\frac{Q}{HP} \approx \frac{K\Delta T}{(RT\mu)^{.75}(PVB)^{.25}}$$

by rearranging and assuming T to be constant

(4) $$\frac{Q}{HP} \approx \frac{1}{Pr}\left(\frac{\mu}{M.W.}\right)^{1/4}\left(\frac{1}{HP_S\ B^2}\right)^{1/4}$$

where

M. W. is molecular wt.

HP_S is specific horsepower - hp/in^3

Pr is Prandtl number, $\frac{\mu C_p}{k}$.

The heat rejection characteristics of two engines can be compared as follows:

When specific power and displacement are equal but working fluids are different:

(5) $$\frac{(Q/HP)_{ENGINE\ a}}{(Q/HP)_{ENGINE\ b}} = \frac{Pr_b}{Pr_a}\left(\frac{\mu_a}{\mu_b}\frac{M.W._a}{M.W._b}\right)^{.25}$$

When working fluids are the same but engine displacement or specific power are different

(6) $$\frac{(Q/HP)_{ENGINE\ a}}{(Q/HP)_{ENGINE\ b}} = \left(\frac{HP_{S\ b}}{HP_{S\ a}}\right)^{.25}\left(\frac{B_b}{B_a}\right)^{.50}$$

A comparison between the heat rejection characteristics of the Vickers Hydrox engine and a conventional air-breathing engine can be made using equations (5) and (6). In the Hydrox engine the working fluid is primarily hydrogen and in the air breather the fluid is mostly air.

The Hydrox engine has 1.5" bore and $HP_S = 2$ and a typical modern air-breathing engine has a 3.34" bore with a HP_S of .5 and a Q/HP = .413.

Thus:

$$\left(\frac{Q}{HP}\right)_{HYDROX} = \left(\frac{Q}{HP}\right)_{AIR}\left(\frac{\mu_{H_2}}{\mu_{AIR}}\frac{MW_{AIR}}{MW_{H_2}}\right)^{.25}\left(\frac{HP_{S\,AIR}}{HP_{S\,H_2}}\right)^{.25}\left(\frac{B_{AIR}}{B_{H_2}}\right)^{.5}$$

$$= .413\left(\frac{.069}{.139}\,\frac{29}{2}\right)^{.25}\left(\frac{.5}{2}\right)^{.25}\left(\frac{3.34}{1.5}\right)^{.5}$$

= .413 x 1.64 x .707 x 1.495 = 0.715

with thermal transport properties evaluated at an assumed average temperature of 3000° F.

A similar analysis can be made for a Hydrox engine operating on a stoichiometric ratio of hydrogen and oxygen. In this case the working fluid is steam. It can be shown that the heat rejection characteristics (Q/HP) would be 40% lower than that of an engine operating on pure hydrogen, as assumed in the previous analysis. Thus there is a convincing indication that significant reduction in heat transfer to the cylinder can be achieved in Hydrox engines as more nearly stoichiometric operation is approached.

Note that the preceding discussion assumes no insulation on the Hydrox engine. Effective thermal insulation should reduce heat rejection appreciably (perhaps as much as 50%).

The above analysis is based on the heat rejection characteristics of the new Willys 6-230 (as reported in SAE Paper 532A) engine which has about the lowest heat rejection of any air-breathing engine reported to date. However, it should be noted that other automotive engines of similar size reject two to three times as much heat as the Willys engine, which indicates that low heat transfer characteristics can be achieved with judicious design and development.

Included as Appendix A in this report are the derivations and results of the cycle analysis with the effects of heat rejection shown. A portion of this analysis was shown and discussed in the August 1962 progress report.

CONTROLS

A. Evaluation of Engine and Propellant Source Configuration and Operating Characteristics

As a result of engine parameter studies, a set of engine equations suitable for use in control system analysis has been agreed upon. These equations describe the power output and the exhaust gas temperature of the engine in terms of the O_2/H_2 mixture ratio and the rate of fuel consumption. A method of throttling the engine was selected, valve sizes and characteristics were estimated and a set of system equations was written. This set of equations was used in setting-up an analog of the system on the Vickers analog computer.

A study of the system by these various methods indicates that the engine power must be regulated at very high rates of response in order to keep speed constant, therefore fuel flow must also be controlled at high response rates. In order to keep cylinder temperature at a desired level during transients, the high response rate is required for both fuel and oxidizer. The present control system configuration reflects these requirements by placing the control valves close to the engine and supplying gases to the valve from a small storage volume held to a relatively constant pressure (see Fig. 9). This almost eliminates problems associated with compressor response. An alternate configuration (see Fig. 10) for the oxygen supply will be investigated in which the oxygen compressor response is kept high by eliminating as much line volume as possible, thus allowing the oxygen to be controlled upstream of the compressor.

Further investigation of the moment of inertia has shown that effects of the engine combustion and torque cycle place certain restrictions on the minimum rotating moment of inertia of the system. Based upon the computed moment of inertia, an undesirable speed variation would occur at 66 cps. Computations indicate that an increase in inertia by a factor of 4 would be required. This change in inertia is designated as the "required moment of inertia" on Figures 6, 7, and 8. It is not anticipated that a flywheel will be required to realize this change in the system since larger diameter generator designs are evolving which will increase the inertia.

B. Evaluation of Control Configuration

The analog computer mechanization which was established was checked for agreement with results obtained from linear analysis. Several hundred data points have been run. The data indicates that the conclusions reached in last month's report are correct.

Three system approaches have been used in this analysis which were described in the August Progress Report. These systems are listed below for reference purposes.

System 1 - Error signal proportional to load change.
System 2 - Error signal proportional to speed.
System 3 - Similar to 2 with more complex compensation.

The system error is plotted as a function of loop gain. In designing a system, a specific value of loop gain would be chosen from the data. The actual system loop gain would vary around this specified nominal value, possibly twenty percent, due to system

Fig. 6 -- ENGINE CONTROL CHARACTERISTIC

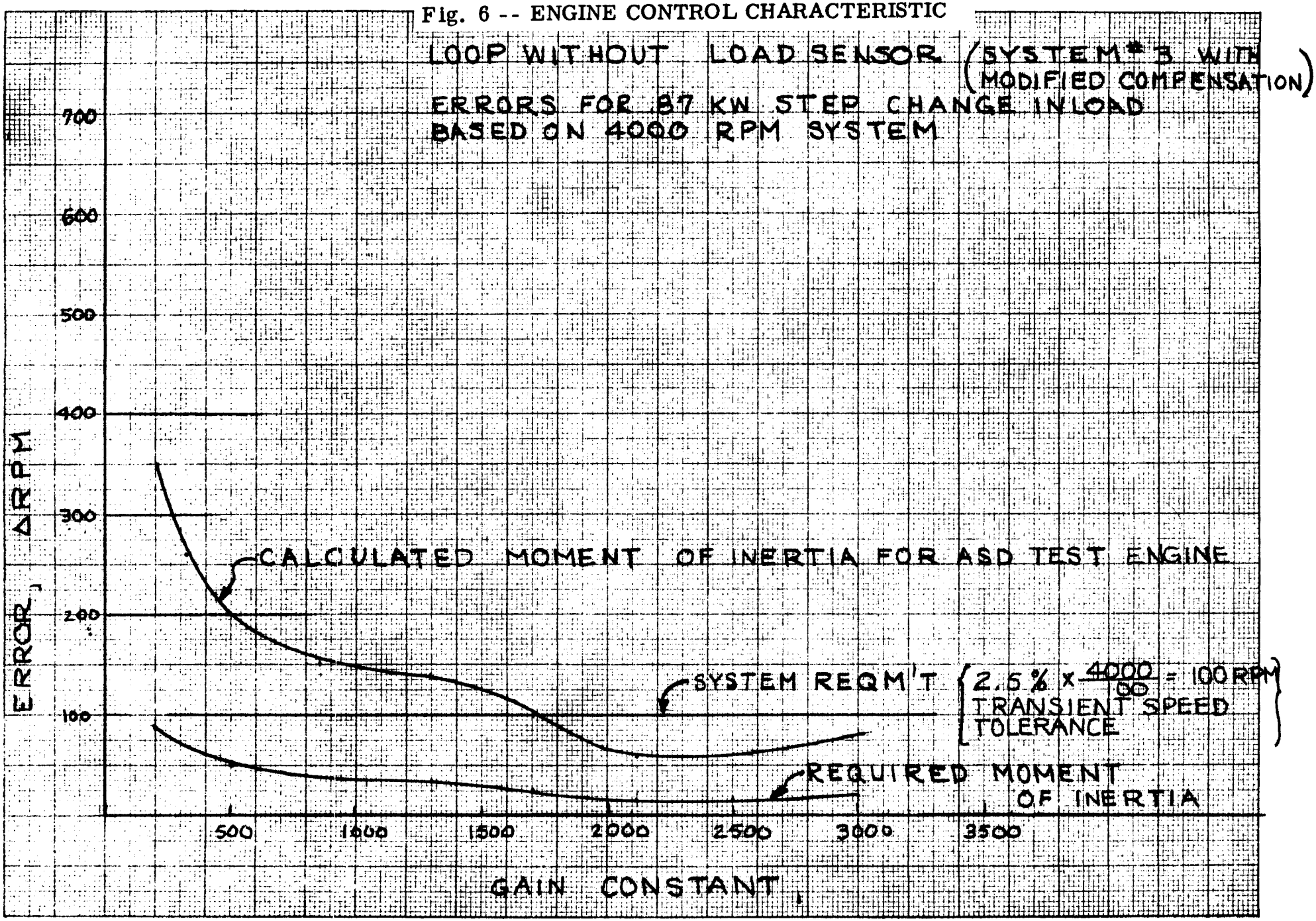

Fig. 7 -- ENGINE CONTROL CHARACTERISTIC

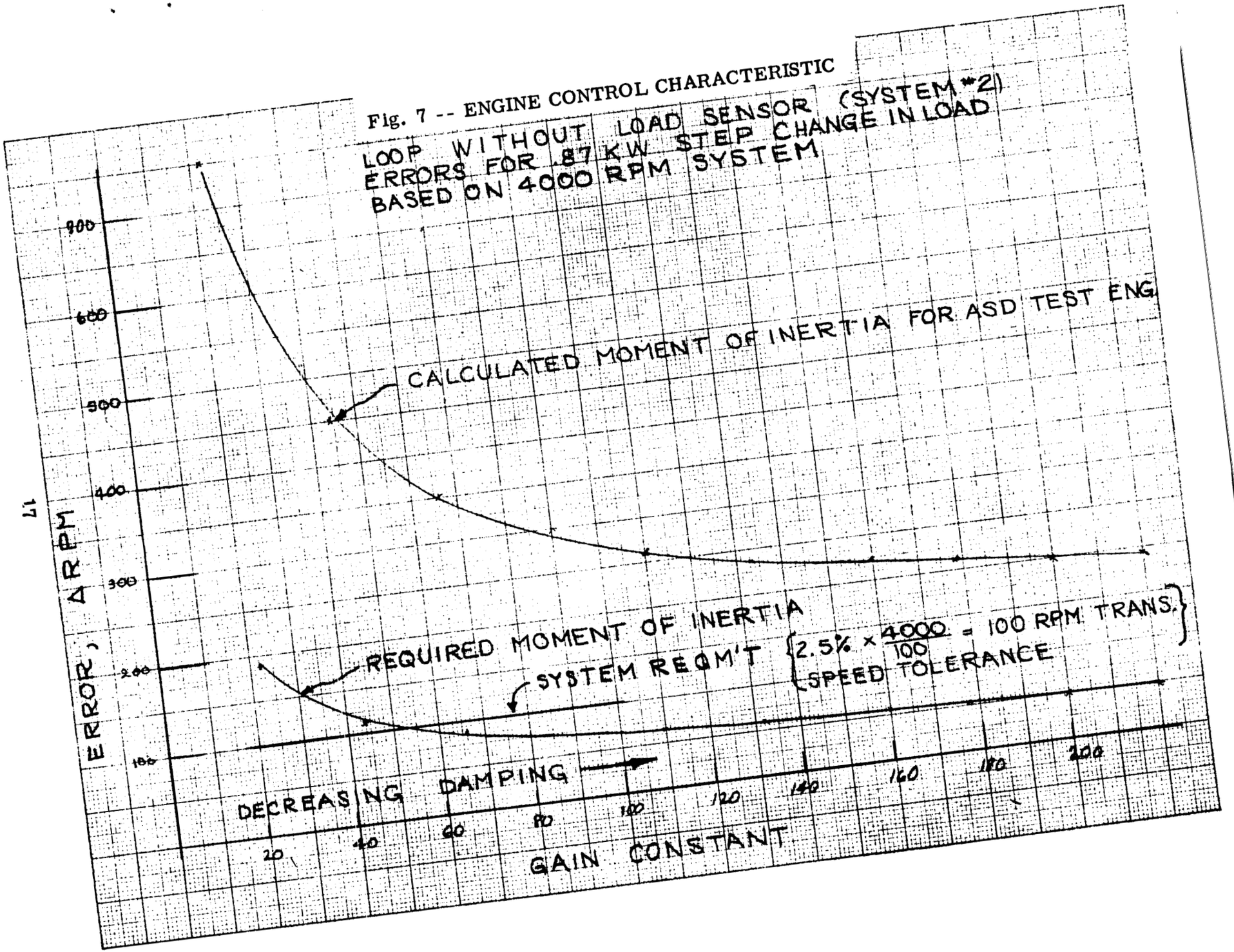

Fig. 8 -- ENGINE CONTROL CHARACTERISTIC

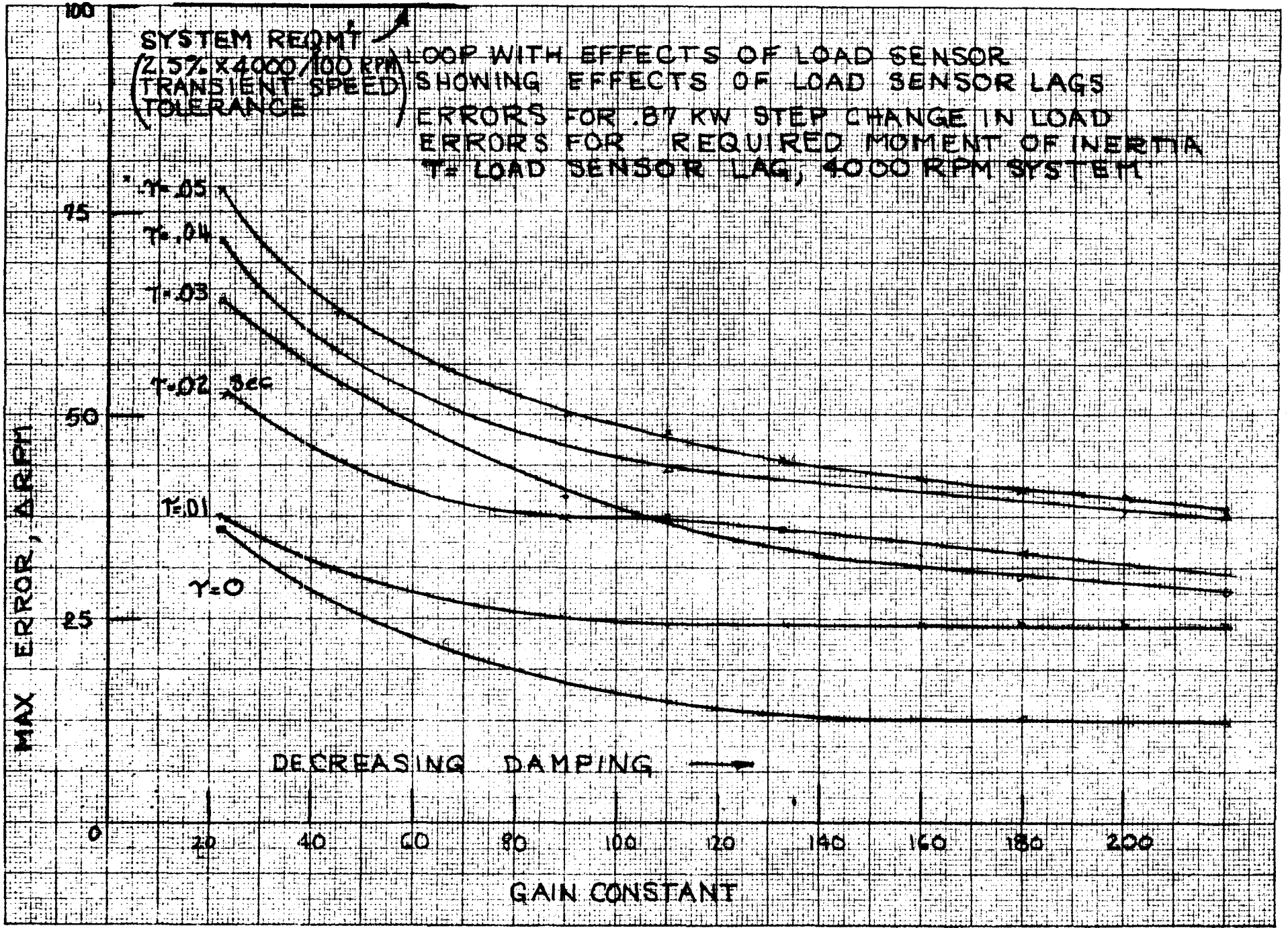

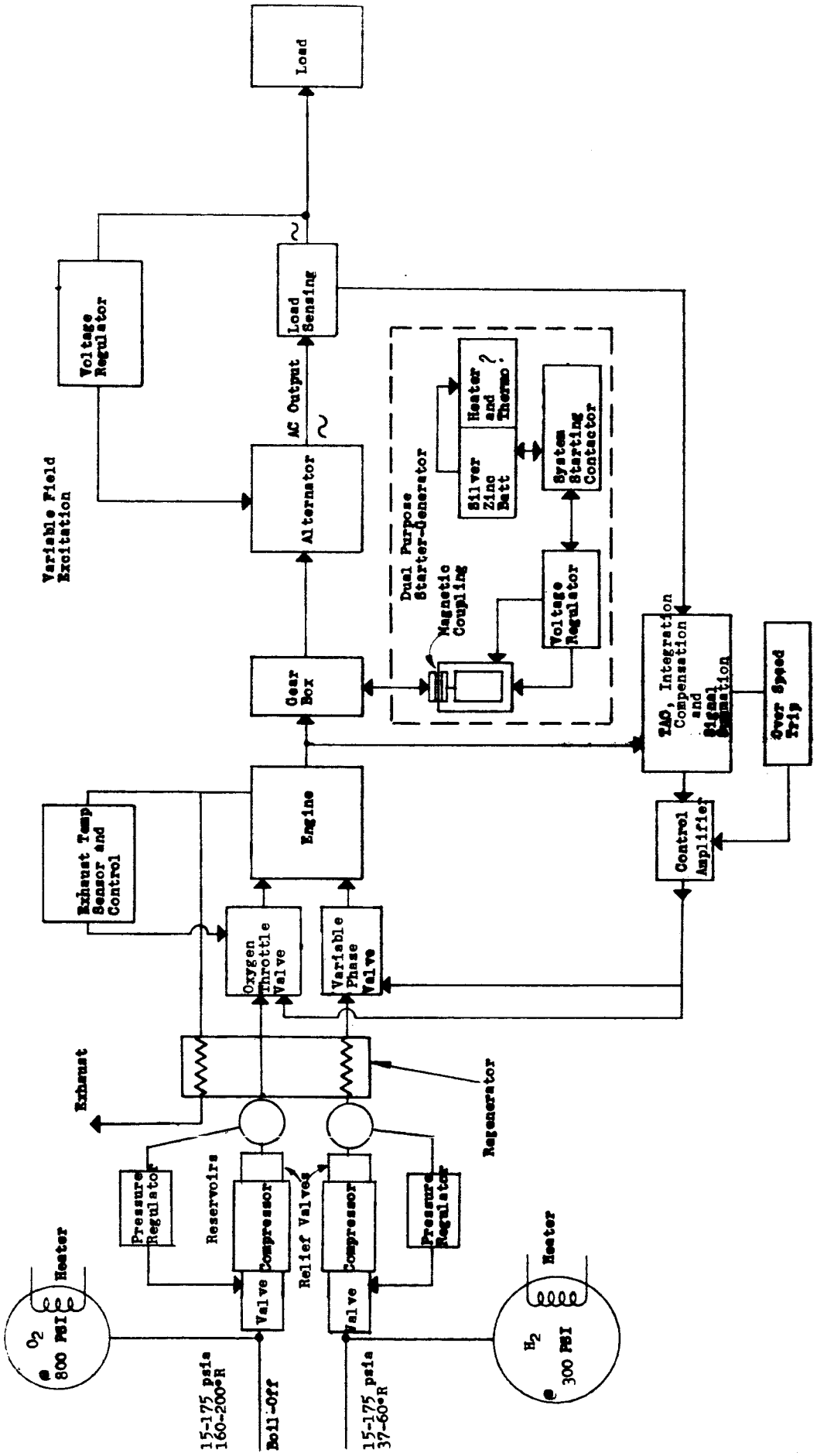

Fig. 9 -- SYSTEM BLOCK DIAGRAM - PRIMARY APPROACH

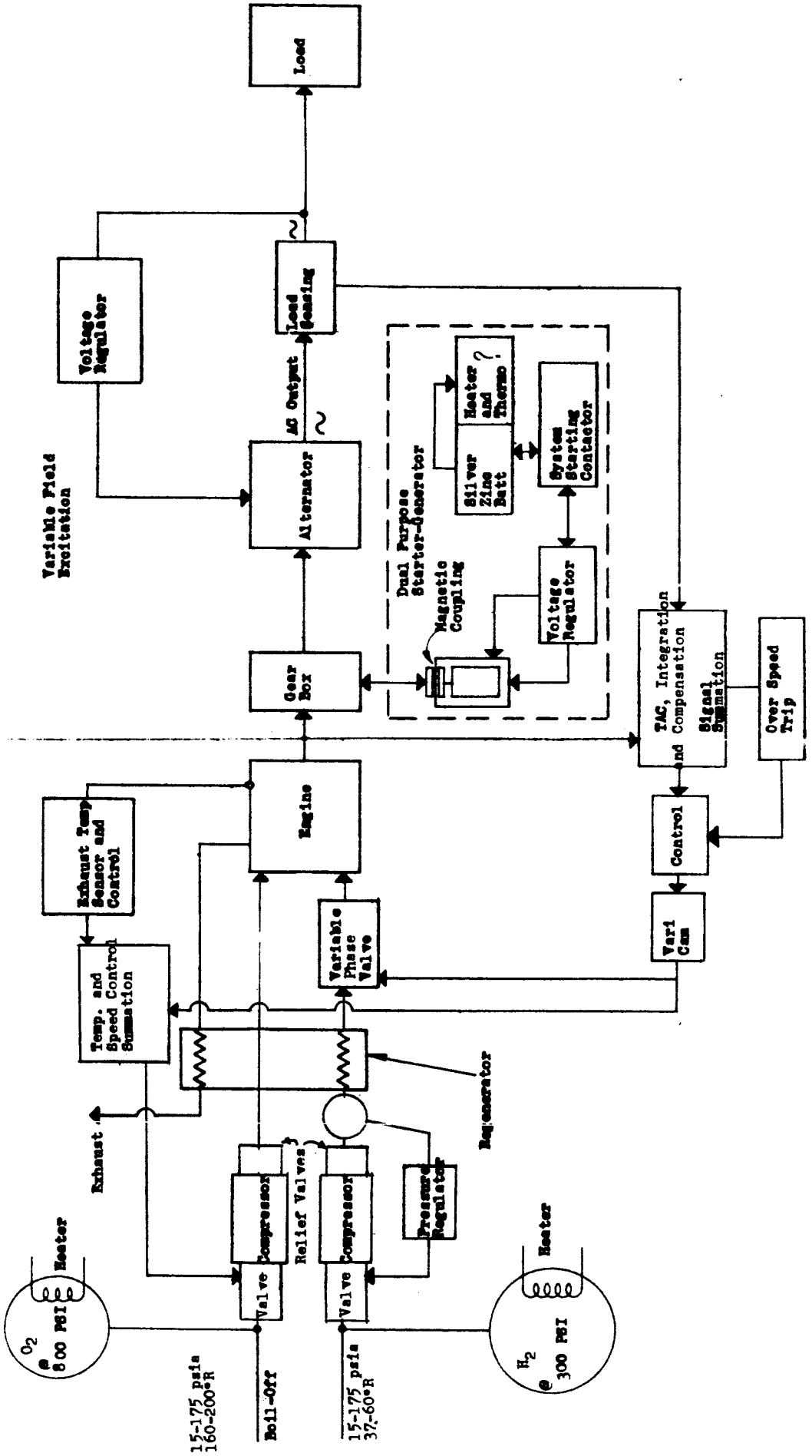

Fig. 10 -- SYSTEM BLOCK DIAGRAM - ALTERNATE APPROACH

non-linearities. This would represent a band of loop gains on the data presented, over which the system accuracy and response should meet requirements. Figure 7 shows system errors for System 2 as a function of loop gain. Note the decrease in error due to the increase in system inertia.

Figure 8 shows the effect of load sensor on the system. (System 1 plus 2). The indications are that, with the load sensor, control requirements can be met with some margin.

Figure 6 shows the result of System 3, although a more optimized compensation function was used to obtain this data. The advantages of this system, when compared with Fig. 7, appear as a reduction in transient error. Since Systems 1 plus 2 have adequate capability to maintain system accuracy, and System 3 represents added complexity, it will not be considered as a primary system approach at this time.

C. Evaluation of Control Components

The selection of components is being based upon general requirements such as:

1. Compatibility with power sources.
2. Compatibility with input and output requirements.
3. Efficiency.
4. Weight and reliability.
5. Ability to meet accuracy and computation requirements.
6. Cost and required development.

Estimates will be made of the amount of torque required to move the valve phasing mechanism at the required response, thus

determining what type of "muscle" will be necessary to provide this function. The other valves will probably require less torque and be more compatible with electrical torque motor applications.

Future Effort - An analytical work statement has been written for the remainder of the study. The major areas listed in this statement are:

1. Obtain system data.
2. Expand analog simulation.
3. Expand linear analysis (90% completed now).
4. Obtain analog data.
5. Write report.

In the next month, effort will primarily involve obtaining data from the expanded analog simulation.

ELECTRICAL COMPONENTS

Work accomplished during September covered analytical and quantitative calculations of alternator designs to meet the electrical output and efficiency goals of the system.

The attached chart shows the parameters of three alternator speeds corresponding to 4, 8, and 12 pole Vickers designs. The efficiencies shown are based on a temperature rise of 40°C in the rotor, or the rotating element, of the machine over ambient at 20°C. with a rotor cooling medium of hydrogen at 7 psi absolute. Stator temperature rise is limited to 30°C through external liquid and/or hydrogen cooling.

Total efficiencies are further based on voltage regulator efficiency of 70% and excitation source efficiency of 70%. Gear train efficiency, if a gearbox is used, is estimated to be 99%. Weights shown are for active electro-magnetic materials only. Depending on the final packaging techniques, and the method of excitation, the total machine weights will be 7 to 15 lbs. over the weights shown for active materials. Lengths will be increased proportionately.

DESIGN PARAMETERS - 400 CYCLE ALTERNATOR

3.0 KVA – 75% POWER FACTOR

MACHINE PARAMETERS ACTIVE MATERIALS ONLY	SPEED-RPM 12000	6000	4000
① NUMBER OF POLES	4	8	12
② MAIN STATOR LAMINATION - O.D.	5.5"	8.0"	10.0"
③ " " LENGTH	3.5"	1.5"	1.5"
④ MAIN ROTOR – O.D	3.23"	5.48"	7.73"
⑤ " " LENGTH	3.75"	1.625"	1.75"
⑥ * " " WEIGHT	7.1 LBS	8.2 LBS.	16.0 LBS
⑦ TOTAL WEIGHT - ACTIVE MATERIALS	25.4 LBS	19.35 LBS	28.2 LBS
⑧ " EFFICIENCY IN HYDROGEN AT 7 P.S.I., INCLUDING EXCITATION AT 60°C	90.5%	91%	91%

* ADD WEIGHT OF SHAFT AND GEARS FOR INERTIA CALCULATIONS

RELIABILITY STUDIES

In September, reliability effort consisted mainly of locating documents containing suitable failure rate information. This information will be useful for reliability estimates of the system components throughout the study contract. Numerous failure rate manuals for mechanical and electrical devices of all types are now at the disposal of Vickers reliability engineering. Applicable manuals obtained thus far include those developed by Boeing Airplane Company, North American Aviation, Martin Marietta Corp., Aerojet General Corp., Radio Corp. of America, and the Rome Air Development Center.

To date, no reliability estimates have been made. The principle reason for this is the lack of a firm system design. In some cases, types of components are not established and in all cases the necessary specifications are not yet determined. For example, alternator failure rates cannot correctly be estimated until basic features such as stator diameter, number of brushes or slip rings, load requirements, etc., are firmed. However, design and types of components are gradually being determined and initial failure rate estimates for certain components will be submitted in later progress reports.

The tentative program for the reliability effort is as follows:

1. Estimate MTBF for significant components.
2. Failure Analysis.
3. Determine redundancy requirements.
4. Recommend fail-safe techniques.

This schedule may be altered somewhat depending on the progress of the development group. In general, reliability effort will be limited initially and will increase as the system design becomes more definitive.

It is expected that the Hydrox engine will have the highest failure rate of the major system components. The ability to establish a valid estimate for it will be very important. Since engines of identical configuration are non-existent, the procedure of estimation is through comparison with other internal combustion engines of similar power levels. Interpolation may be used to obtain the expected failure rates. Letters have been sent to the Department of Air Force, Navy and several government contractors requesting appropriate engine failure rate data.

MATERIALS

Recommendations from NASA on oxygen injector materials are given in Reference 2.

From the standpoint of fabricability, machinability, availability, and utility at both intermediate (1600°F) and high temperatures (2000°F), it appears that Rene' 41, Haynes 25, Inconel 702, and Haynes metal-ceramic LT-1 possess elevated temperature properties equivalent or superior to those outlined in the NASA recommendations.

Mechanical properties of these alloys are as follows:

1. Rene' 41 - Nickel Base
   Oxidation resistant up to, and including 1800°F.

Yield Strength @ 1800°F		33,000 psi	
Stress-rupture @	1650°F	100 hours	21,000 psi
	1650°F	500 hours	14,000 psi
	1800°F	100 hours	9,500 psi

2. Haynes 25 - Cobalt Base
   Oxidation resistant up to 2000°F

Yield strength @ 1800°F		23,000 psi	
Stress-rupture @	1600°F	100 hours	18,000 psi
	1800°F	100 hours	7,500 psi

   1000 hours required to produce .73% creep @ 1500°F at a stress of 14,000 psi.

3. 702 Inconel - Nickel Base
   Oxidation resistant to 2300°F

Yield strength @ 1600°F		30,000 psi	
Stress-rupture @	1600°F	100 hours	9,000 psi
	1800°F	100 hours	4,000 psi

4. Haynes Metal-Ceramic - 77% CR 23% $A_{L_2} O_3$

   Good thermal shock resistance and oxidation. It is superior to LT-1B at 2200°F and above.

   The expansion coefficient is approximately the same as LT-1B.

HYDROGEN COMPRESSOR

The final design assembly drawing of the experimental

hydrogen compressor was given in the August progress report. All design drawings have been released to the shop for fabrication of an experimental unit. Parts are now being manufactured. Fabrication is about 30% complete.

A schematic of the planned hydrogen compressor test circuit is shown in Fig. 11. As shown the circuit will allow testing on either saturated nitrogen vapor, hydrogen gas cooled to liquid nitrogen temperature, or saturated hydrogen vapor.

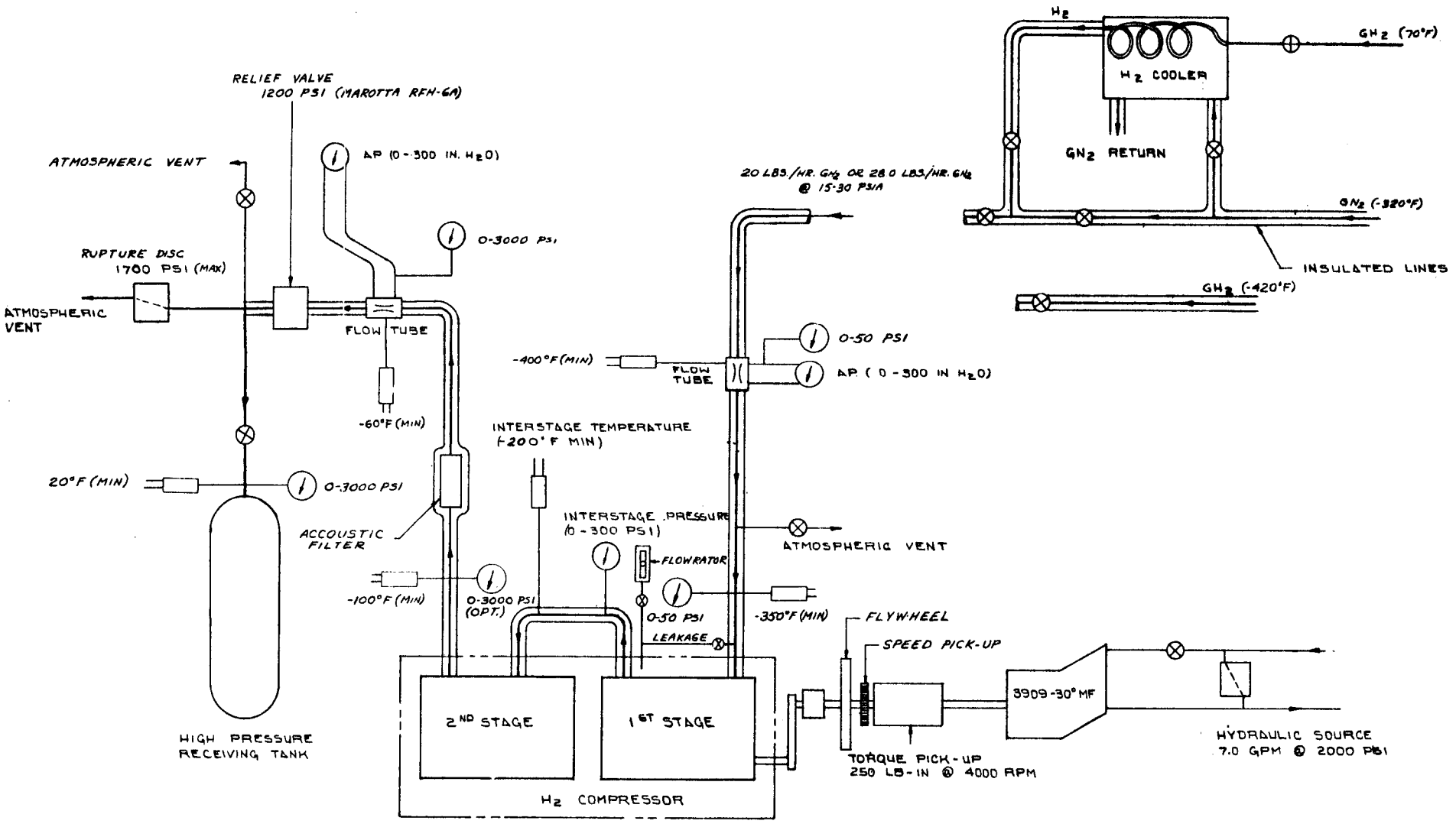

Fig. 11 - TEST CIRCUIT - H_2 COMPRESSOR

REGENERATOR

Enough preliminary design analysis has been completed on the regenerator to furnish an idea of the basic design problems which will be encountered. A schematic of the regenerator is shown in Fig. 12. A cross counterflow heat exchanger in which hydrogen at cryogenic temperature and high pressure is warmed by the engine exhaust is planned. (The actual configuration could be circular or annular instead of rectangular for packaging purposes). The following decisions have been made as a result of the analysis to date:

1. Engine exhaust heat will be regenerated to the incoming hydrogen only. Oxygen will be raised to a convenient temperature level.

2. A plenum chamber between the exhaust manifold and the regenerator will not be used, since there already is considerable volume in the regenerator and resonance effects may be of benefit.

3. A relatively large and simple regenerator using commercial tubing will be designed for operation at sea level exhaust pressure. This regenerator will be built and tested to evaluate heat transfer coefficients and icing problems.

   The analysis is presented in Figures 13 and 14. The assumptions used in this analysis are as follows:

Fig.12

SCHEMATIC:

CROSS-COUNTER FLOW

HYDROX ENGINE REGENERATOR

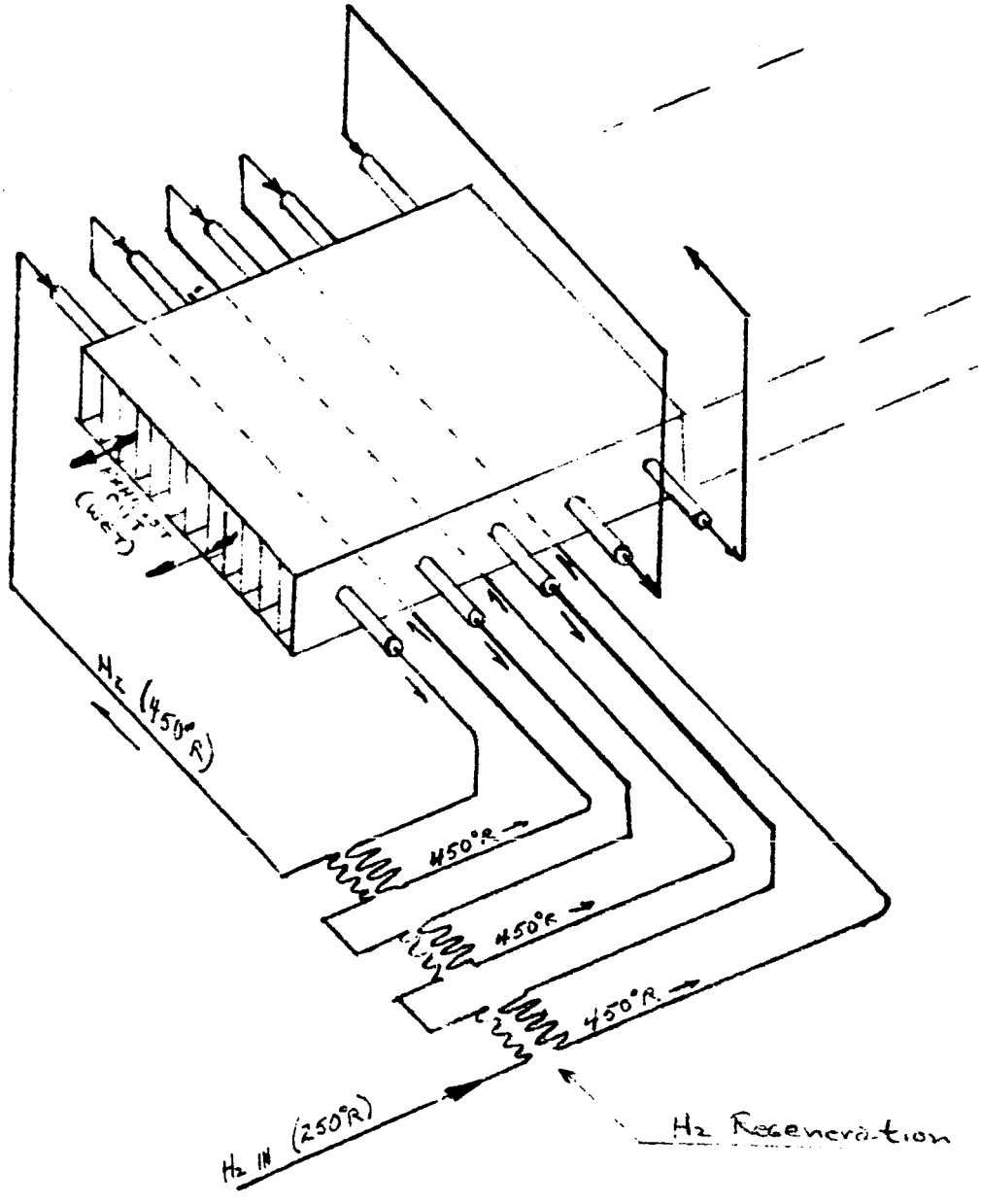

a. A square wave flow pulse is assumed in which the entire flow occurs for 10% of the cycle. Zero flow and zero heat transfer occurs over the rest of the cycle. Heat transfer coefficients and pressure drops are calculated for steady flow at the Reynolds numbers and Mach numbers of the pulse.

b. The exhaust temperature (Tex = 1540°R) is the mass average exhaust temperature computed over the portion of the cycle in which exhaust ports are open. See reference 3 page 167 for a discussion of this temperature.

c. The effects of resonance are omitted. The heat transfer coefficient could increase by a factor of ten if a standing wave were set up in the exhaust flow, perpetuating the engine pulsations. Such resonance effects are difficult to initiate or predict.

The exhaust film coefficient is the controlling factor due to the low density and velocity of exhaust flow. Fig. 13 gives the exhaust flow area as a function of exhaust surface density for two regenerator lengths. A surface density of 250 $ft.^2/ft.^3$ is attainable with commercial tubing. It can be seen that a drastic reduction in size is possible with flight weight hardware. It must also be emphasized that these calculations are very conservative, and that reliable heat transfer data does not exist in our flow regime. Hence, the need for an operating regenerator.

The major unknowns at present are the effects of part load operation on icing and the best procedure to follow in system warm-up. Investigation of these matters will continue.

Fig. 13 Flow Area Vs Surface Density for $L < \begin{matrix} 2.0\ ft \\ 1.0\ ft \end{matrix}$, Hydrox Engine Regenerator

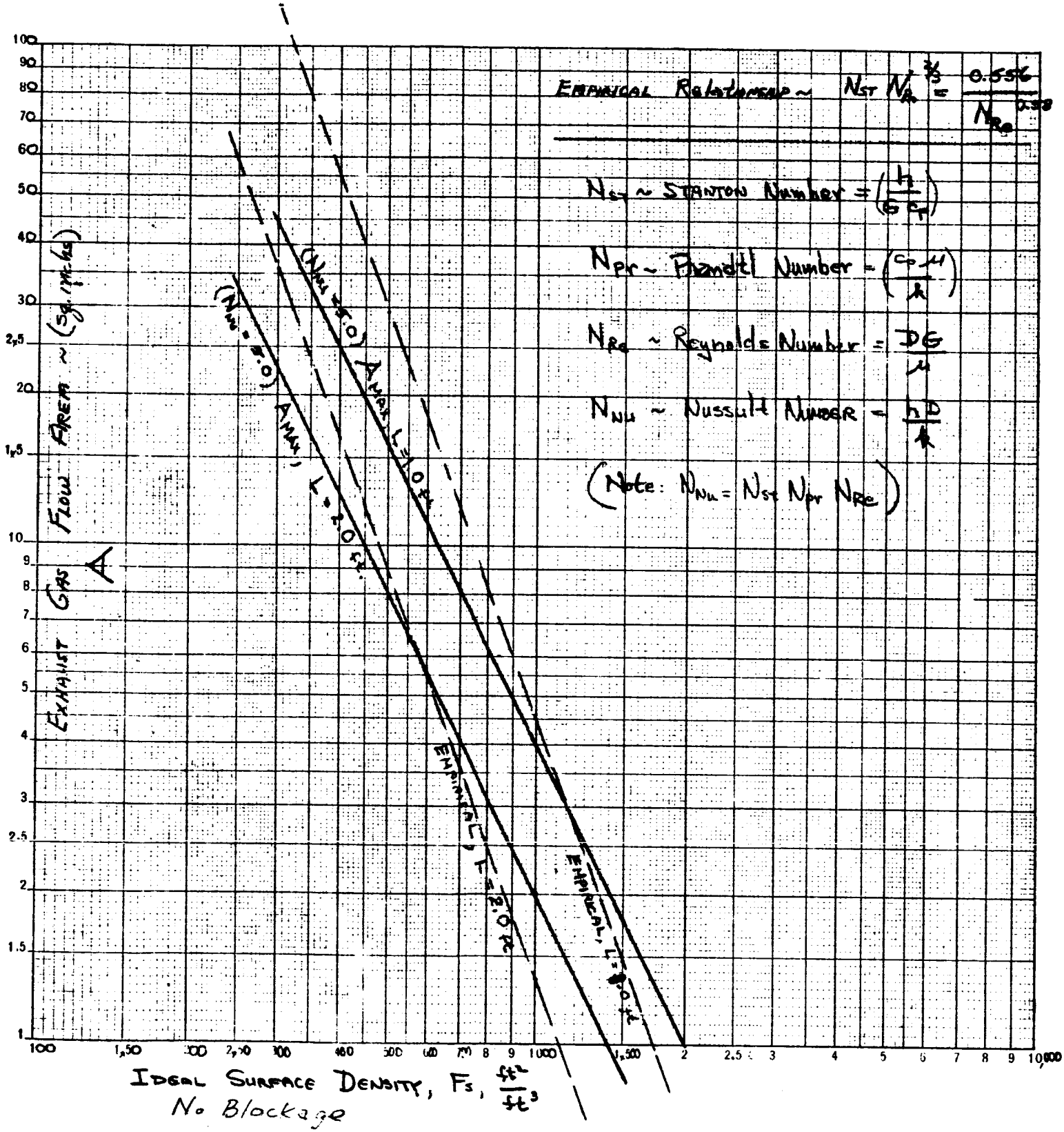

Fig. 14

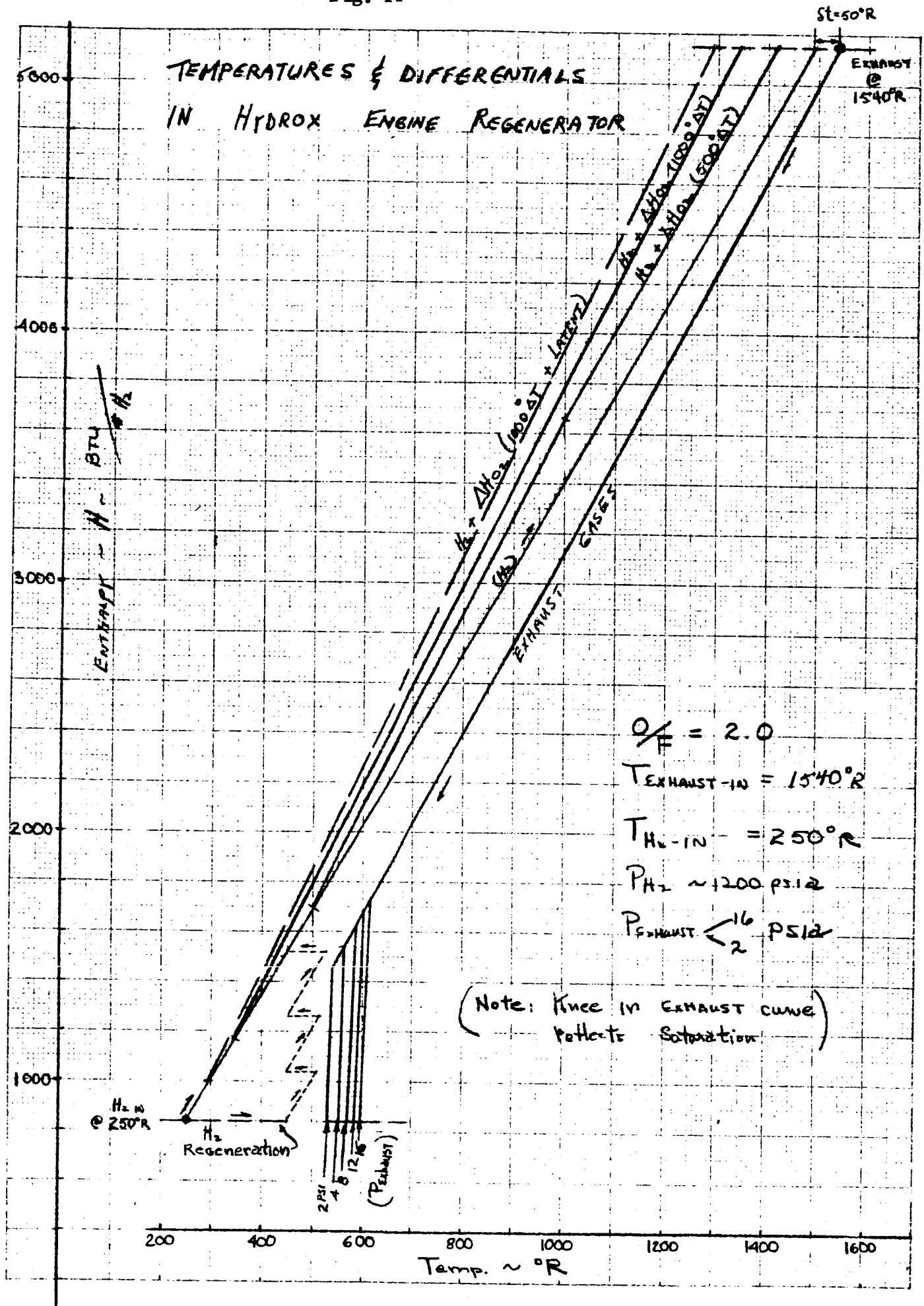
TEMPERATURES & DIFFERENTIALS
IN HYDROX ENGINE REGENERATOR
St=50°R
EXHAUST @ 1540°R
ENTHALPY - H ~ BTU
5000
4000
3000
2000
1000
0
H₂ + ΔHOx (1000°ΔT + LATENT)
H₂ + ΔHOx (1000°ΔT)
H₂ + ΔHOx (500°ΔT)
(H₂) =
EXHAUST GASES
O/F = 2.0
T EXHAUST-IN = 1540°R
T H₂-IN = 250°R
P H₂ ~ 1200 PSIA
P EXHAUST 16 / 2 PSIA
(Note: Knee in Exhaust curve reflects Saturation)
H₂ IN @ 250°R
H₂ Regeneration
2 PSI
4
8
12
(P EXHAUST)
200
400
600
800
1000
1200
1400
1600
Temp. ~ °R

Although the final system design may not include exhaust heat regeneration to the oxygen, it is planned to provide for oxygen regeneration in the experimental regenerator. This will provide the necessary flexibility to evaluate regenerator performance with and without oxygen regeneration.

ENGINE

The engine being constructed for this program is essentially identical to the engine constructed under the ASD contracts. Design modifications and improvements are discussed in the August 1962 progress report. Parts for the engine are now being fabricated and are about 25% complete.

OXYGEN INJECTOR

The oxygen injector configuration shown in Fig. 11 of the August progress report is being built. Some results of calculations which were made to determine torsional tube wall thickness are shown in Figures 15 and 16. In Fig. 15, stress as a function of wall thickness is shown, and in Fig. 16, the cam follower force and cam follower Hertz stress are shown vs. tube wall thickness. The dotted line at .008" represents the thickness chosen. It is believed that fatigue considerations can be satisfied at this stress level. (1000 hours life is the design goal).

Injector drawings have been released and the injector construction is approximately 25% complete. A materials change from Inconel 702 to Inconel 718 or Rene' 41 has been made due to the lack of availability of Inconel 702.

PROBLEM AREAS

No problem areas beyond those originally anticipated for this program have been encountered during this report period. The schedule has been slightly delayed on the engine and regenerator effort.

Fig. 15

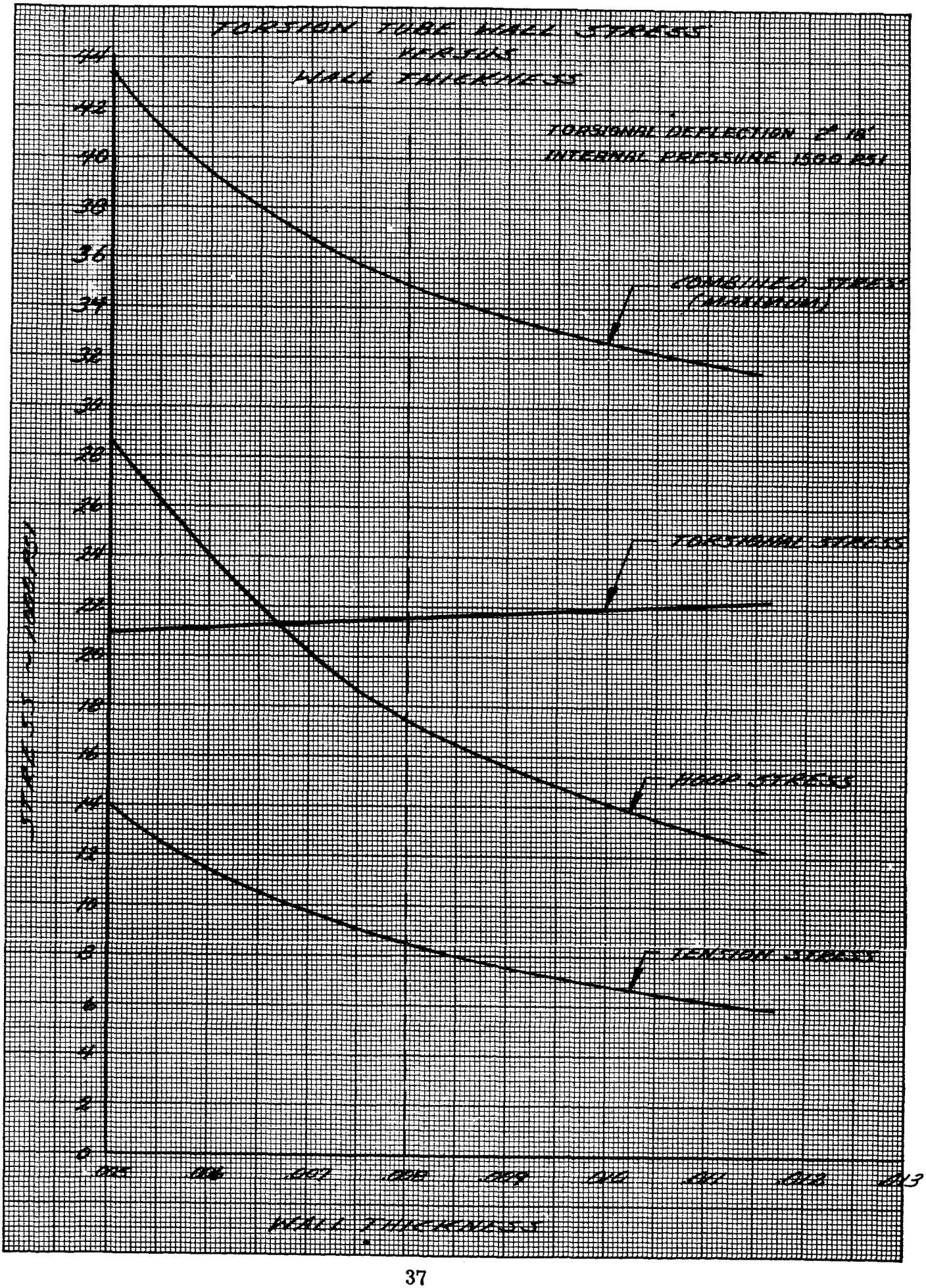
TORSION TUBE WALL STRESS
LONGITUDINAL
WALL THICKNESS
TORSIONAL DEFLECTION 2° IN
INTERNAL PRESSURE 1500 PSI
COMBINED STRESS
(CALCULATED)
TORSIONAL STRESS
HOOP STRESS
TENSION STRESS
WALL THICKNESS

Fig. 16

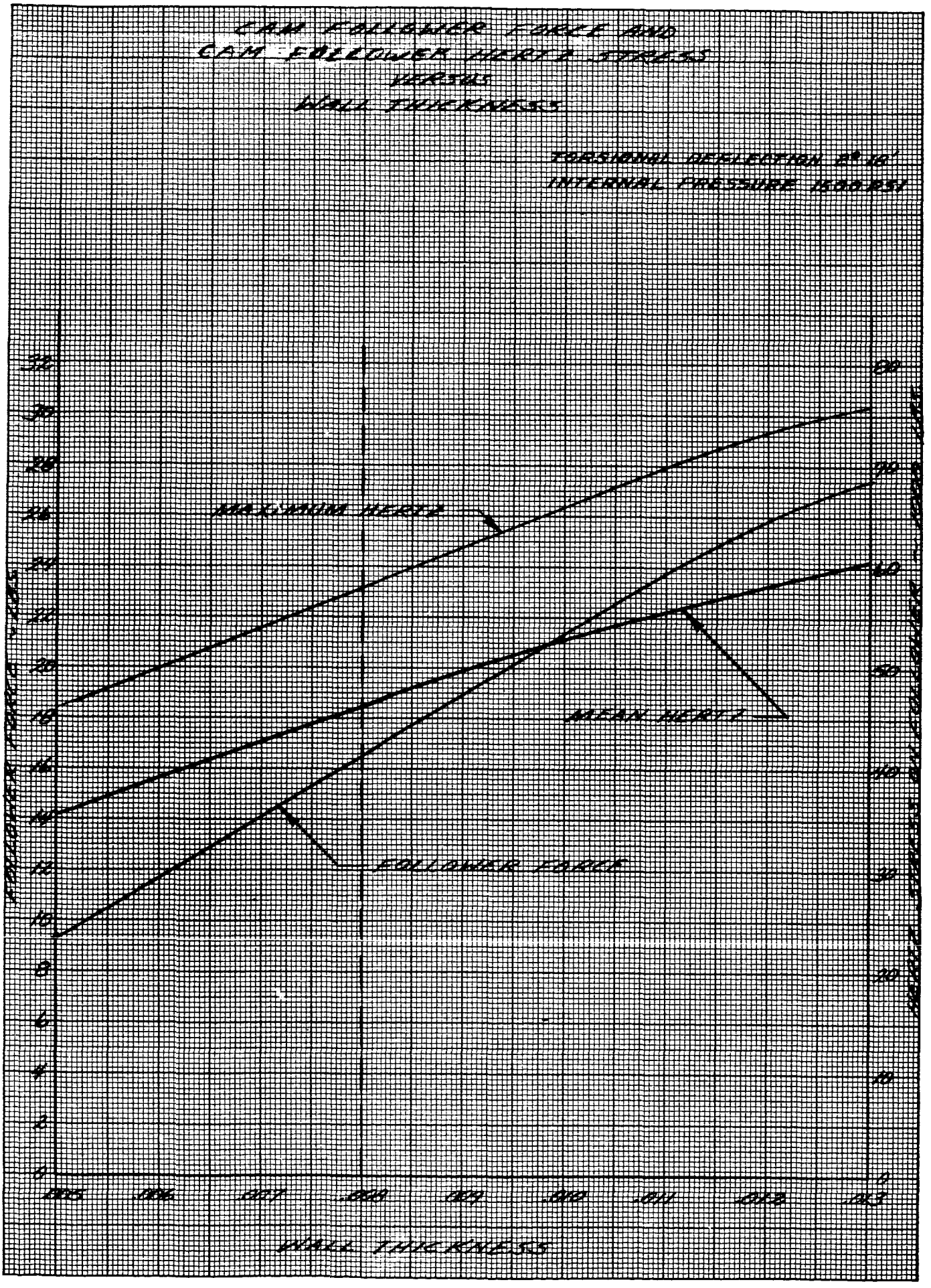
CAM FOLLOWER FORCE AND
CAM FOLLOWER HERTZ STRESS
VERSUS
ROLL THICKNESS
TORSIONAL DEFLECTION 2° 16'
INTERNAL PRESSURE 15000 PSI
MAXIMUM HERTZ
MEAN HERTZ
FOLLOWER FORCE
ROLL THICKNESS

PLANNED FUTURE WORK

For the forthcoming report period it is planned to continue work in all of the areas of the program as indicated in the schedule in Fig. 1. Parametric studies, controls analysis, and selection of electrical components will continue. Reliability and failure analysis will continue and material studies will continue as required for selection of materials for the experimental components. Fabrication of all experimental components will continue.

An analysis of engine dynamics will be completed during the next time period. The linear controls analysis will be completed and data will be obtained from the expanded analog simulation. The work statement mentioned in the controls analysis will be followed. Component design studies will be initiated. This involves conceptual layout and design studies of the flight weight engine and associated hardware.

REFERENCES

1. ASD Technical Report 61-327, Vol. II, "Study of Integrated Cryogenic Fueled Power Generating and Environmental Control Systems - Cryogenic Tankage Investigation."

2. NASA Lewis memo dated 12 September 1962.

3. Taylor, C. F., and Taylor, E. S., The Internal Combustion Engine, 2nd edition.

APPENDIX

Regenerative Power Cycles With Heat Loss

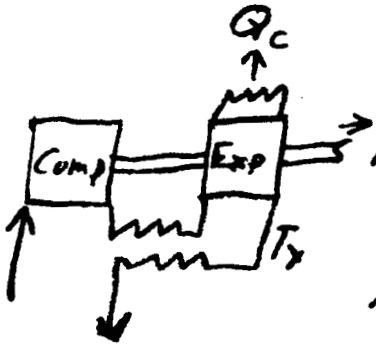

Compression function may be liquid pump.

η_∞ describes expander performance when $Q_c = 0$

T_x is held constant

η_1 is cycle performance with $Q_c = 0$

$$X = \frac{Q_c}{HP_x}$$

$$\eta_x = \frac{HP_x}{\frac{HP_1}{\eta_1} + Q_c + (HP_x - HP_1)} = \frac{HP_x/HP_1}{\frac{1}{\eta_1} + (X+1)\frac{HP_x}{HP_1} - 1}$$

With T_x held constant, $\frac{HP_x}{HP_1} \geq 1$ as $0 < X$. The most conservative assumption is $\frac{HP_x}{HP_1} = 1$, $\eta_x = \frac{\eta_1}{1 + X\eta_1}$

This is equivalent to assuming that all waste heat is extracted before the expansion process, and is <u>too conservative</u>.

$$HP_x = HP_1 + (Q_c + HP_x - HP_1)\, y\, M_\infty$$

$$0 < y < 1.0$$

If $y = 1$, all heat has been extracted after expansion.

$$\frac{HP_x}{HP_1} = \frac{1 - y M_\infty}{1 - (x+1) y M_\infty}$$

$$\eta_x = \frac{1}{\left(\frac{1}{\eta_1} - 1\right) \frac{1 - y(x+1) M_\infty}{1 - y M_\infty} + x + 1}$$

In most cycles of interest,

$.40 < M_\infty < .50$, and $.40 < M_1 < .55$

The term x is best interpreted as the heat rejection which cannot be regenerated.

Since M_∞ and M_1 are nearly equal, a value of $y = 1$ would imply no influence of x on η_x.

In evaluating y, we should remember that η_∞ includes a friction loss which is part of the heat rejection that behaves like exhaust heat extraction. From automotive data, a value of $y = 0.60$ is suggested. Using $\eta_\infty = .45$,

$$\eta_x = \frac{1}{\left(\frac{1}{\eta_1} - 1\right)\frac{1 - .27(x+1)}{.73} + x + 1}$$

If $\eta_1 = .50$, $x = 1.0$,

$$\eta_x = 0.38$$

Whereas, if $y = 0$ or 1.0

$$\eta_x = 0.333 \text{ or } 0.458$$

The values of x and y need test evaluation!

Summary:

$$\eta_x = \frac{}{\left(\frac{1}{\eta_1} - 1\right) HP_1/HP_x + x + 1}$$

If $HP_x/HP_1 = 1.0$,

$$\eta_x = \frac{1}{\frac{1}{\eta_1} + x}$$

$$HP_x/HP_1 = \frac{1}{1 - \frac{x}{\frac{1}{y\eta_\infty} - 1}}$$

$$\eta_x = \frac{1}{\left(\frac{1}{\eta_1} - 1\right)\left(1 - \frac{x}{\frac{1}{y\eta_\infty} - 1}\right) + x + 1}$$

Plot $\eta_x = f(\eta_1, x, y\eta_\infty)$

η_1 < 0.55 to 0.4 $\quad$ x < 1.2 to .2

$y\eta_\infty = 0.3, 0.4, 0.5$

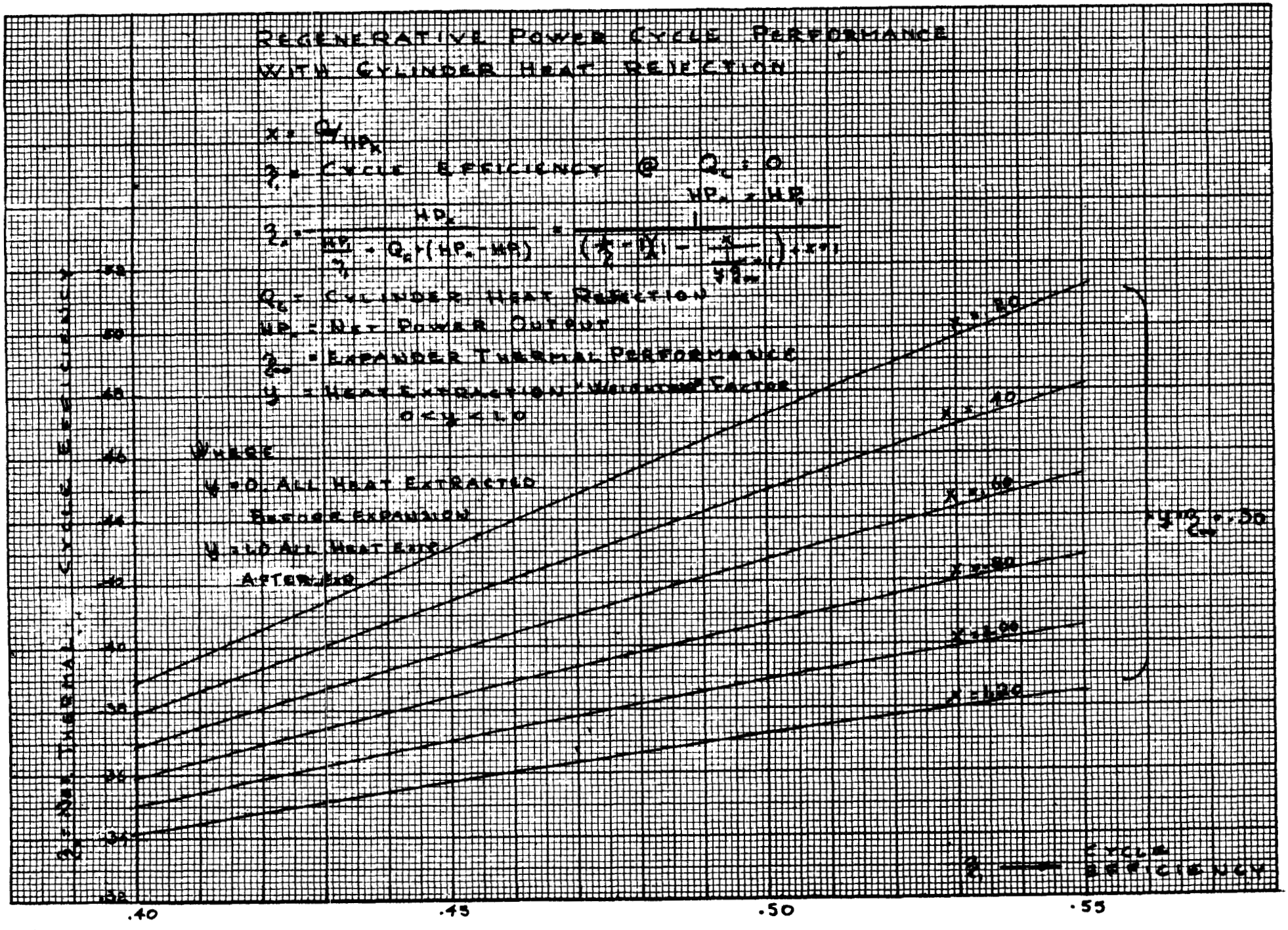
REGENERATIVE POWER CYCLE PERFORMANCE
WITH CYLINDER HEAT REJECTION
$X = \frac{Q_{HP_x}}{HP_x}$
η_x = CYCLE EFFICIENCY @ $Q_c = 0$
$\eta_x = \frac{HP_x}{\frac{HP_x}{\eta_x} + Q_R(HP_x - HP_x)} = \frac{1}{\left(\frac{1}{\eta_x} - Y\left(1 - \frac{X}{\eta_x \eta_{ex}}\right)\right)(1-Y)}$
Q_R = CYLINDER HEAT REJECTION
HP_x = NET POWER OUTPUT
η_{ex} = EXPANDER THERMAL PERFORMANCE
Y = HEAT EXTRACTION / REGENERATOR FACTOR
$0 < Y < 1.0$
WHERE
Y = 0 ALL HEAT EXTRACTED BEFORE EXPANSION
Y = 1.0 ALL HEAT EXTRACTED AFTER EXP.
X = 80
X = 40
X = 60
X = 30
X = 20
X = 120
$\eta_{ex} = .50$
η_x — CYCLE EFFICIENCY
.40
.45
.50
.55

A-5

HW 736

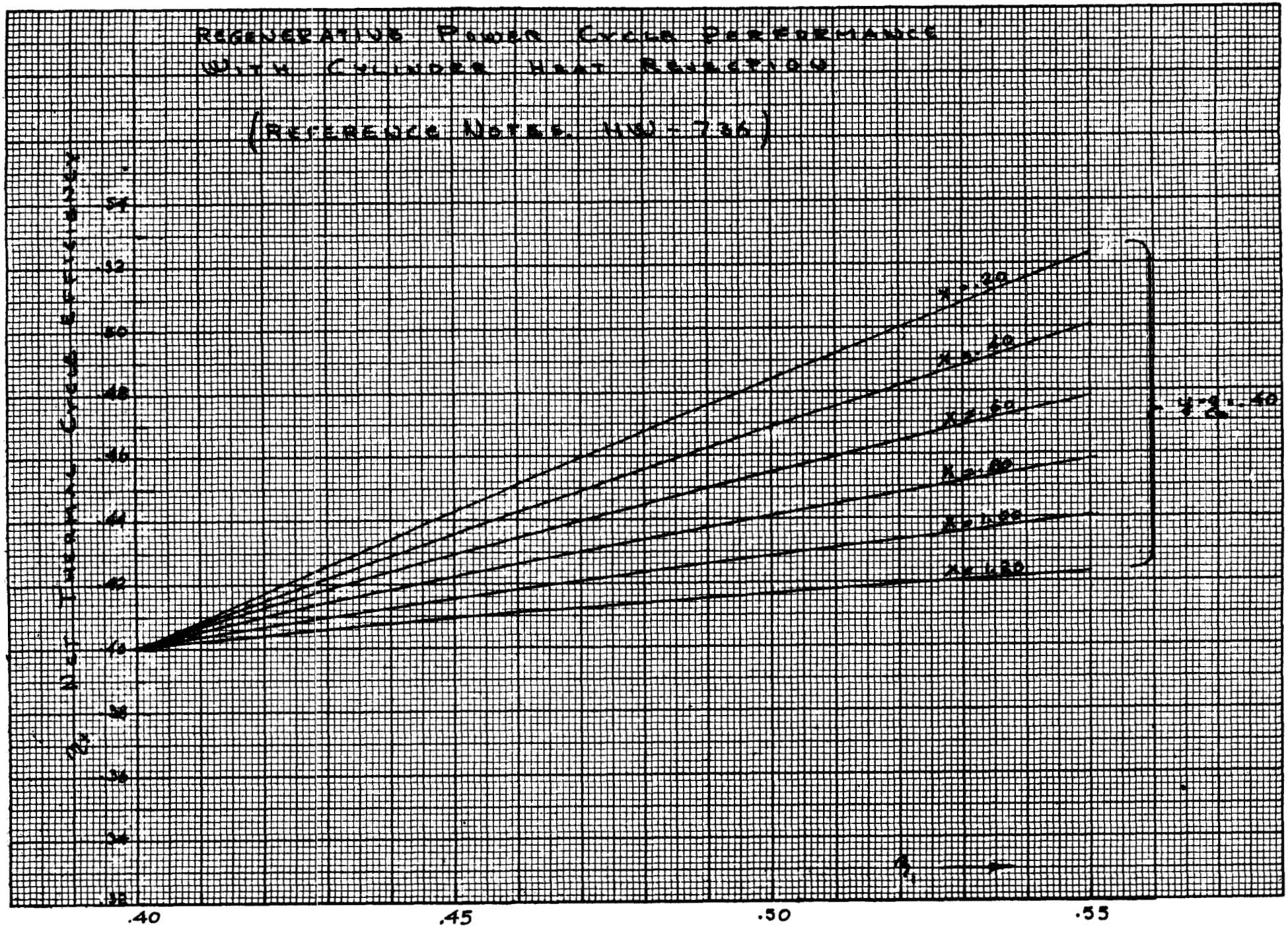
REGENERATIVE POWER CYCLE PERFORMANCE
WITH CYLINDER HEAT REJECTION
(REFERENCE NOTES, HW-7336)
Engine Efficiency, Percent
54
52
50
48
46
44
42
40
38
36
34
32
X = .20
X = .30
X = .40
X = .50
X = .60
X = .80
X = 1.00
X = 1.50
$\eta_1 - \eta_2 = .40$
.40
.45
.50
.55
η_1

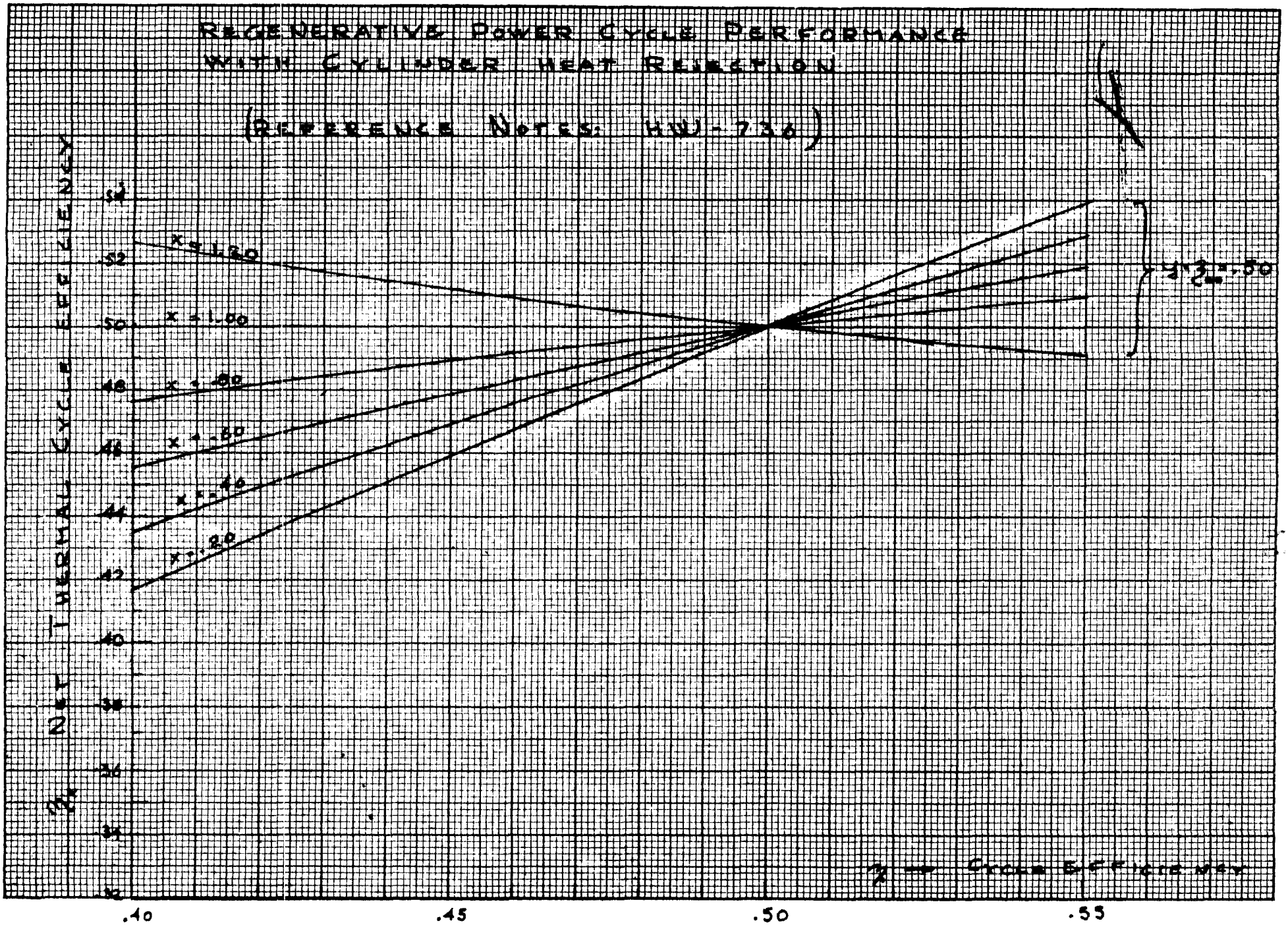
REGENERATIVE POWER CYCLE PERFORMANCE
WITH CYLINDER HEAT REJECTION
(REFERENCE NOTES: HW-7386)
x = 1.20
x = 1.00
x = .80
x = .60
x = .40
x = .20
$\frac{T_3}{T_2} = .50$
54
52
50
48
46
44
42
40
38
36
34
32
.40
.45
.50
.55
η — Cycle Efficiency